The importance of including local correlation times in the calculation of inter-proton distances from NMR measurements: ignoring local correlation times leads to significant errors in the conformational analysis of the Glcα1–2Glcα linkage by NMR spectroscopy

Mukram Mackeen,[a] Andrew Almond,[b] Ian Cumpstey,[c] Seth C. Enis,[c] Eriks Kupce,[d] Terry D. Butters,[a] Antony J. Fairbanks,[c] Raymond A. Dwek[a] and Mark R. Wormald[a]

Received 20th March 2006, Accepted 31st March 2006
First published as an Advance Article on the web 2nd May 2006
DOI: 10.1039/b604126d

The experimental determination of oligosaccharide conformations has traditionally used cross-linkage ^{1}H–^{1}H NOE/ROEs. As relatively few NOEs are observed, to provide sufficient conformational constraints this method relies on: accurate quantification of NOE intensities (positive constraints); analysis of absent NOEs (negative constraints); and hence calculation of inter-proton distances using the two-spin approximation. We have compared the results obtained by using ^{1}H 2D NOESY, ROESY and T-ROESY experiments at 500 and 700 MHz to determine the conformation of the terminal Glcα1–2Glcα linkage in a dodecasaccharide and a related tetrasaccharide. For the tetrasaccharide, the NOESY and ROESY spectra produced the same qualitative pattern of linkage cross-peaks but the quantitative pattern, the relative peak intensities, was different. For the dodecasaccharide, the NOESY and ROESY spectra at 500 MHz produced a different qualitative pattern of linkage cross-peaks, with fewer peaks in the NOESY spectrum. At 700 MHz, the NOESY and ROESY spectra of the dodecasaccharide produced the same qualitative pattern of peaks, but again the relative peak intensities were different. These differences are due to very significant differences in the local correlation times for different proton pairs across this glycosidic linkage. The local correlation time for each proton pair was measured using the ratio of the NOESY and T-ROESY cross-relaxation rates, leaving the NOESY and ROESY as independent data sets for calculating the inter-proton distances. The inter-proton distances calculated including the effects of differences in local correlation times give much more consistent results.

Introduction

The intensity of a NOESY cross-peak is a function of the cross-relaxation rate between the pair of dipolar coupled nuclei, which depends upon their separation and molecular motion.[1] The reorientation of the inter-nuclear vector can be approximated for some molecules by a single correlation time (τ_c); for rigid molecules it is the rate of isotropic molecular tumbling. For small oligosaccharides, such as tetrasaccharides, NOESY cross-peak intensities are typically observed to be close to zero in high-field spectrometers. This is because $\omega_o\tau_c \approx 1.12$ (ω_o is the Larmor frequency), the point at which NOEs are theoretically predicted to be zero according to the Lipari–Szabo formalism. In these cases, the use of negative NOE constraints becomes ambiguous. However, the rotating frame NOE (ROE) can still be measured as this is positive for all values of τ_c.[2] ROESY cross-peak intensities are significantly smaller than their NOESY equivalent for larger oligosaccharides, where $\omega_o\tau_c \gg 1.12$, making ROESY cross-peaks less easy to observe and less accurate to quantify. The implementation of the ROESY experiment also has significant problems that have limited its applicability. In particular, it is susceptible to Hartmann–Hahn (TOCSY) transfers through scalar couplings.[3] These can be suppressed by a weak and/or off-resonance spin-locked field,[4,5] but this is difficult to implement in practice when the chemical shift difference between scalar-coupled spins is small,[6,7] as is frequently the case for oligosaccharides. A more successful practical approach to removing Hartmann–Hahn effects is the transverse-ROESY (T-ROESY) experiment.[8,9] It has been demonstrated that the signal to noise ratio of one-dimensional T-ROESY spectra is at least as good as of ROESY spectra for tetrasaccharides, while allowing effective removal of artefacts.[10] However, in all these cases the assumption is usually made that different proton pairs across a specific glycosidic linkage have similar effective correlation times. This allows a simple r^{-6} dependence of the NOE/ROE to be used with a calibration NOE/ROE to calculate inter-proton distances.[11,12]

We have used NOESY, ROESY and T-ROESY spectra at 500 MHz and 700 MHz to look at the Glcα1–2Glcα linkage, found in the triglucosylated cap of $Glc_3Man_9GlcNAc_2$, in a

[a]*Oxford Glycobiology Institute, Department of Biochemistry, University of Oxford, South Parks Road, Oxford, UK OX1 3QU. E-mail: mark@glycob.ox.ac.uk; Fax: +44 (0)1865 275738; Tel: +44 (0)1865 275738*
[b]*Faculty of Life Sciences, University of Manchester, Manchester Interdisciplinary Biocenter, Princess Street, Manchester, UK M1 7ND*
[c]*Chemistry Research Laboratory, Department of Chemistry, University of Oxford, South Parks Road, Oxford, UK OX1 3TA*
[d]*Varian NMR Systems, The Magnet Technology Centre, 6 Mead Road, Oxford Industrial Park, Yarnton, Oxon, UK OX5 1QU*

small (Glc_3Man*O*Me) and medium sized ($Glc_3Man_7GlcNAc_2$) oligosaccharide. Glucosylated oligomannose oligosaccharides are involved in a number of important steps during the biosynthesis and folding of glycoproteins,[13,14] including: (i) the *N*-glycosylation of the nascent peptide chain in the endoplasmic reticulum (ER) lumen, involving transfer of $Glc_3Man_9GlcNAc_2$ to the peptide by the oligosaccharyltransferase (OST) complex; (ii) the initial steps of glycan processing on the glycoprotein in the ER, involving removal of the terminal glucose residue from $Glc_3Man_9GlcNAc_2$ by α-glucosidase I and from $Glc_2Man_9GlcNAc_2$ and $Glc_1Man_9GlcNAc_2$ by α-glucosidase II; and (iii) the chaperone dependent folding of glycoproteins in the ER, involving recognition of $Glc_1Man_9GlcNAc_2$ by proteins such as calnexin and calreticulin and reglucosylation of $Man_9GlcNAc_2$. The conformation of the glucosyl (Glc_x) caps is critical for recognition at each stage of this process. The presence and absence of cross-linkage NOEs can be interpreted in terms of positive and negative conformational constraints respectively, and thus used to define glycosidic linkage conformations.[15,16] Only a few NOEs are observed across most glycosidic linkages, so conformational analysis depends critically upon accurate quantitative analysis of both positive (cross-peak present) and negative (cross-peak absent) constraints.

We show that assuming that all the proton pairs across the Glcα1–2Glcα linkage have similar correlation times leads to very significant differences in the distances calculated for the different experiments and the different samples. Using the ratio of NOESY to T-ROESY cross-relaxation rates allows the correlation time to be measured for each proton pair. When these differences in local correlation times are included in the calculation of the distances from the NOESY and ROESY data, a much more consistent set of results is obtained.

Results

^{1}H NMR resonance assignments of the Glcα1-2Glcα1-3Glcα1-3Manα moiety of Glc_3Man*O*Me and $Glc_3Man_7GlcNAc_2$ (Fig. 1) have been previously reported.[17,18] These were confirmed and, in the case of $Glc_3Man_7GlcNAc_2$, extended to a complete assignment.

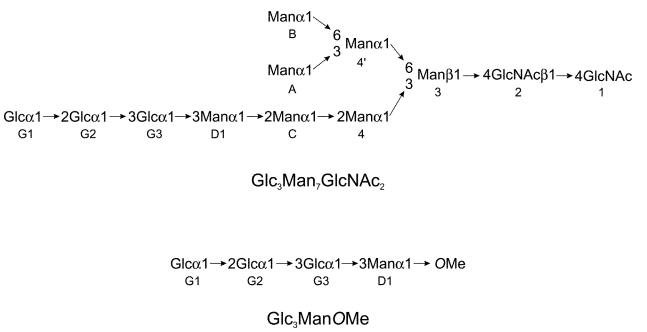

Fig. 1 Schematic representation of the $Glc_3Man_7GlcNAc_2$ and Glc_3Man*O*Me structures showing the primary sequence and residue numbering.

Comparison of the NOESY and ROESY results at 500 MHz

NOESY, ROESY with weak and strong spin-lock fields, and T-ROESY spectra were recorded on both samples at 500 MHz (see Materials and methods for details). Traces through the G1:H1 peak, in F2, are shown for Glc_3Man*O*Me (Fig. 2) and $Glc_3Man_7GlcNAc_2$ (Fig. 3). These NOEs/ROEs form the basis of determining the conformation of the Glcα1–2Glcα (G1–G2) linkage. The cross-peak volumes are given in Table 2.

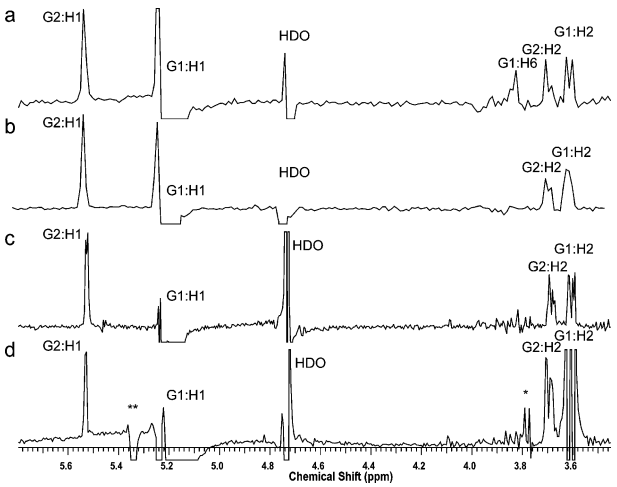

Fig. 2 Traces through the G1:H1 peak, parallel to F2, of the 500 MHz 2D ^{1}H NMR spectra of Glc_3Man*O*Me in D_2O at a mixing time of 200 ms; (a) strong spin-lock ROESY; (b) weak spin-lock ROESY; (c) T-ROESY; (d) NOESY (sample concentration five times that used in a–c). * = edge of a peak with maximum in different trace. ** = spectral artefact.

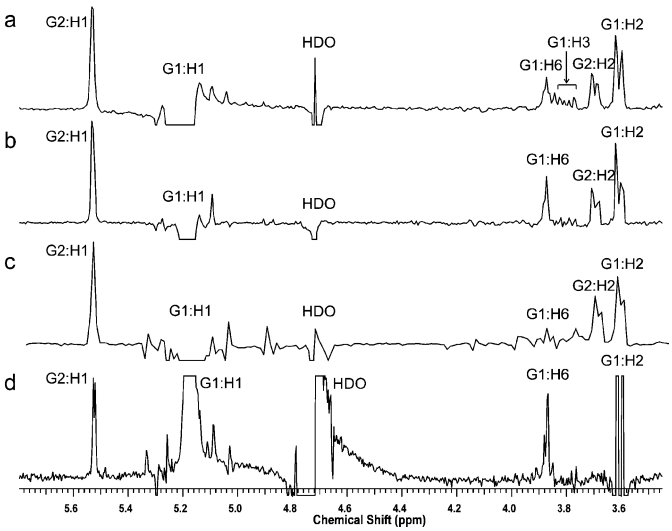

Fig. 3 Traces through the G1:H1 diagonal peak, parallel to F2, of the 500 MHz 2D ^{1}H NMR spectra of $Glc_3Man_7GlcNAc_2$ in D_2O at a mixing time of 200 ms; (a) strong spin-lock ROESY; (b) weak spin-lock ROESY; (c) T-ROESY; (d) NOESY.

Glc_3Man*O*Me gives positive NOESY peaks (*i.e.* opposite sign to the diagonal peaks, Fig. 2d) at 500 MHz as expected for a molecule of low molecular weight and thus short correlation time. The signal-to-noise ratio is very poor for the NOESY spectrum, presumably because $\omega_o\tau_c$ is only slightly less than 1.12 (the trace shown in Fig. 2d is at a five-fold increase in sample concentration relative to Fig. 2a–c). The qualitative pattern of cross-peaks is the same for the weak spin-lock ROESY, T-ROESY and NOESY, cross-peaks being seen from G1:H1 to G2:H1 and G2:H2 (Fig. 2b–d). The strong spin-lock ROESY is not as clean, with a number

Table 1 Proton–proton correlation times, τ_{ij}, for Glc_3Man*O*Me and $Glc_3Man_7GlcNAc_2$ calculated from NOESY/T-ROESY cross-relaxation rate ratios[a] (30 °C)

		500 MHz		700 MHz	
Proton pair		σ(NOE)/σ(T-ROE)	τ_{ij}/ps	σ(NOE)/σ(T-ROE)	τ_{ij}/ps
Glc_3Man*O*Me					
G1:H1	G1:H2	0.22	280	—	—
	G2:H1	0.20	289	—	—
	G2:H2	0.48	200	—	—
$Glc_3Man_7GlcNAc_2$					
G1:H1	G1:H2	−0.33	485	−0.64	625
	G2:H1	−0.51	560	−0.72	665
	G2:H2	0.00	360	−0.47	545

[a] Measured using cross peak intensities over diagonal peak intensity at a mixing time of 200 ms.

Table 2 Calculated inter-proton distances based on NOESY and ROESY cross peak volumes using model 1 (rigid isotropic rotor) or model 2 (effective correlation time for each proton pair, see Table 1). nd—cannot be determined

	Proton pair		Cross-peak volume	Calibration distance/Å	Calculated distance/Å (model 1)	τ_{ij}/ps	Calculated distance/Å (model 2)
Glc_3Man*O*Me							
ROESY—500 MHz	G1:H1	G1:H2	1.68	2.3	—	280	—
		G2:H1	1.85		2.26	289	2.27
		G2:H2	0.83		2.59	200	2.49
NOESY—500 MHz	G1:H1	G1:H2	4.84	2.3	—	280	—
		G2:H1	4.9		2.30	289	2.24
		G2:H2	7.67		2.13	200	2.40
$Glc_3Man_7GlcNAc_2$							
ROESY—500 MHz	G1:H1	G1:H2	1.33	2.3	—	485	—
		G2:H1	1.59		2.23	560	2.26
		G2:H2	0.68		2.57	355	2.50
NOESY—500 MHz	G1:H1	G1:H2	0.49	2.3	—	485	—
		G2:H1	0.71		2.16	560	2.32
		G2:H2	not observed		>3.5	360	nd
NOESY—700 MHz	G1:H1	G1:H2	20.19	2.3	—	625	—
		G2:H1	19.5		2.31	665	2.36
		G2:H2	8.78		2.64	545	2.51

of very weak TOCSY peaks being observed between 3.5 and 4.0 ppm (Fig. 2a). There is also a significant G1:H1 to G1:H6/H6′ peak (G1:H6 and G1:H6′ have the same chemical shift). The quantitative comparison of the ROESY and NOESY data is not so satisfactory. In the ROESY spectrum the G1:H1 to G2:H1 cross-peak is significantly larger than the G1:H1 to G2:H2 cross-peak, in the NOESY this is reversed with the G1:H1 to G2:H2 cross-peak being much larger.

$Glc_3Man_7GlcNAc_2$ gives negative NOESY peaks at 500 MHz and a much better signal-to-noise ratio (sample concentration in Fig. 3d is the same as in Fig. 3a–c) than Glc_3Man*O*Me, as expected for a larger molecule with a longer correlation time. However, in this case the qualitative pattern of peaks is significantly different for the NOESY and ROESY spectra. Only one inter-residue peak is seen in the NOESY spectrum (Fig. 3d), the G1:H1 to G2:H1. In the weak spin-lock ROESY and T-ROESY, the G1:H1 to G2:H2 cross-peak is seen as well (Fig. 3b–c). In the strong spin-lock ROESY spectrum, TOCSY peaks are again observed (Fig. 3a). These are more pronounced than in the spectra of Glc_3Man*O*Me due to the stronger spin-lock field used (4.3 kHz instead of 2.8 kHz). The G1:H1 to G1:H6/H6′ cross-peak is clearly seen in all the spectra other than the T-ROESY, where it is only just visible above the noise. As for Glc_3Man*O*Me, the weak spin-lock ROESY and T-ROESY give very similar relative peak volumes.

The absence of a cross-linkage NOESY peak where a ROESY peak is present was also observed for one of the terminal linkages of $Glc_1Man_9GlcNAc_2$ (data not shown).

Comparison of the NOESY and ROESY results on $Glc_3Man_7GlcNAc_2$ at 500 MHz and 700 MHz

The T-ROESY and NOESY spectra of $Glc_3Man_7GlcNAc_2$ at 700 MHz are shown in Fig. 4a and 4b respectively, the equivalent spectra at 500 MHz being Fig. 3c and 3d. There are significant qualitative differences in both spectra at the different field strengths. In the NOESY spectrum at 700 MHz, the G1:H1 to G2:H2 cross-peak is observed, not present at 500 MHz, while the G1:H1 to G1:H6/H6′ peak is much reduced in intensity. In the ROESY spectrum, the G1:H1 to G1:H6/H6′ cross-peak is easily observed.

Determination of effective inter-proton correlation times

The effective correlation times for each proton pair were calculated using the ratio of the NOE build-up rate to the T-ROE build-up rate.[10] This ratio was chosen for two reasons. Firstly, it is a more accurate method of determining correlation times than using either the NOE/ROE ratio or the ROE/T-ROE ratio[10] and secondly this leaves the NOE and ROE as independent data sets for

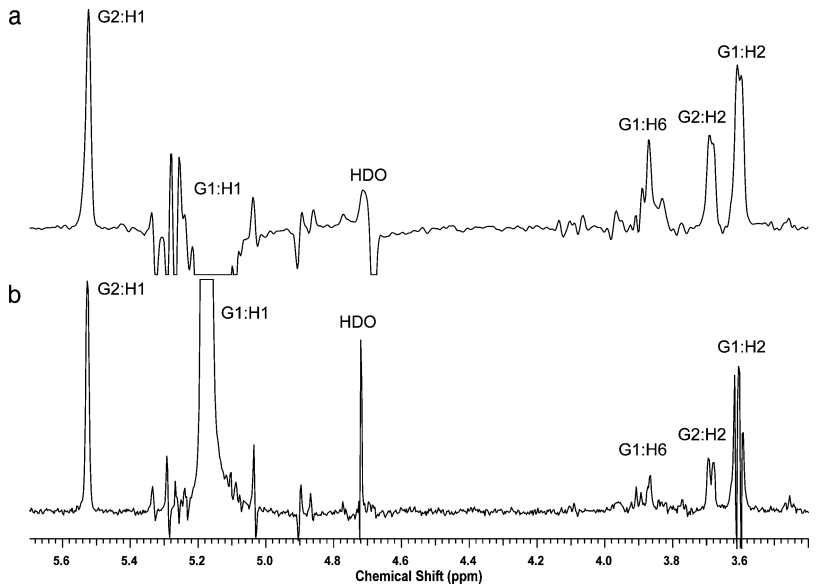

Fig. 4 Traces through the G1:H1 diagonal peak, parallel to F2, of the 700 MHz 2D ^{1}H NMR spectra of $Glc_3Man_7GlcNAc_2$ in D_2O at a mixing time of 200 ms; (a) T-ROESY; (b) NOESY.

calculating the inter-proton distances (see below). The calculated effective correlation times are given in Table 1. As can be seen, there are very significant differences in the correlation times between different proton-pairs across the G1–G2 linkage (up to 35%).

Calculation of inter-proton distance constraints

Inter-proton distance constraints were calculated from the NOE and ROE cross-peak volumes using the intra-residue G1:H1–G1:H2 peak as the internal calibrant. Distances were calculated both by making the usual assumption that all proton-pairs across a given linkage have the same correlation time, model 1, or by using the calculated effective correlation times for each proton pair, model 2 (see methods for details). The NOE and T-ROE data sets cannot be used to calculate independent distances because they have already been used together to calculate the correlation time and thus will produce identical distances using model 2. The results are given in Table 2. An error of ±5% in the measured NOE/ROE intensities relative to the calibrant peak leads to an error of ±0.02 Å in the calculated distances for the stronger NOEs/ROEs, and an error of up to ±0.03 Å in the calculated distances for the weaker NOEs/ROEs. An error of ±10% in the measured NOE/ROE intensities relative to the calibrant peak leads to errors of ±0.03 Å to ±0.06 Å in the calculated distances.

As can be seen in Table 2, there are very significant differences in the distances calculated by model 1 for the same proton pair, much larger than any errors associated with inaccuracies in the experimental measurement. For example the G1:H1–G2:H2 distance in Glc_3Man*O*Me is calculated to be 2.13 Å from the NOESY data at 500 MHz and 2.59 Å from the ROESY data at 500 MHz (consistent with the direct comparison on peak volumes discussed above). These differences are very much smaller using model 2 (2.49 Å *versus* 2.40 Å). Using model 1 the absence of the G1:H1–G2:H2 NOESY peak in $Glc_3Man_7GlcNAc_2$ at 500 MHz is interpreted as a distance greater than the upper limit for NOE observation (taken conservatively to be 3.5 Å), whereas using model 2 the distance is simply undetermined because $\omega_o\tau_c \approx 1.12$. In general, there is better agreement between the distances calculated using model 1 and model 2 for the ROESY data than those calculated for the NOESY data, as would be expected. However, the best agreement is between the distances calculated using model 2 for the ROESY data and for the NOESY data.

Discussion

Both NOESY and ROESY spectra are used in determining glycosidic linkage structures of oligosaccharides. NOESY spectra often give better signal to noise ratios and do not have problems associated with possible TOCSY contamination, and are thus used more frequently for conformational analysis.[12] For Glc_3Man*O*Me, the ROESY spectrum gave the best signal to noise but a spin-lock field of 2.8 kHz produced considerable TOCSY contamination. For $Glc_3Man_7GlcNAc_2$, the NOESY spectrum gave better signal to noise than the ROESY. The T-ROESY spectrum showed no evidence of TOCSY contamination, but the signal to noise was lowest for both compounds.

Measurements on a tetrasaccharide[10] have shown that different proton pairs within the same monosaccharide residue can have slightly different effective correlation times, as can different proton pairs across the same glycosidic linkage, but the biggest differences were observed between proton pairs across different linkages, consistent with the above assumption.

However, we have measured dramatically different effective correlation times for different proton pairs across the Glcα1–2Glcα linkage in both the small and medium sized oligosaccharides (Table 1). Ignoring these differences leads to the calculated inter-proton distances varying significantly depending on (i) whether the spectra were recorded on the tetra- or dodecasaccharide, (ii) whether NOE or ROE data was used, and (iii) whether the spectra

were recorded at 500 MHz or 700 MHz (Table 2, model 1). Including these variations in effective correlation time in the calculation of the inter-proton distances gives much better agreement between the different data (Table 2, model 2). Using model 2, it is clear that the Glcα1–2Glcα linkage shows very similar conformational constraints in both the tetra- and dodecasaccharide, indicating that it adopts the same conformation in both. This method also allows much more precise conformational constraints to be used with confidence either when calculating the structure from the constraints or when using the constraints to compare to molecular modelling results.

Different local correlation times between different proton pairs in the same molecule could arise either from differences in internal flexibility in different regions of the molecule or anisotropic bulk tumbling. In previous NMR studies on $Man_9GlcNAc_2$,[19] the NOE build-up curves for the majority of the structure could be fitted using a single correlation time. However, the NOESY cross-peaks arising from protons in the terminal glycosidic linkages were much weaker, suggesting shorter correlation times. Thus, the internal flexibility of the terminal linkages may be higher than that of internal linkages. When comparing the correlation times for the G1:H1/G2:H1 and G1:H1/G2:H2 proton pairs, these have one proton in common and the second proton is part of a rigid ring. Any contribution of the internal flexibility to the correlation time is due to the flexibility of the Glcα1–2Glcα linkage, and might be expected to be same for both proton pairs. This suggests anisotropic tumbling as a more plausible reason for the differences in effective correlation time. $Glc_3Man_7GlcNAc_2$ is a relatively extended molecule and so isotropic tumbling would not necessarily be expected. Molecular modelling indicates that the inter-nuclear vector of the G1:H1/G2:H2 proton pair (which shows the shortest correlation time and for which no NOE is seen at 500 MHz) is almost perpendicular to the long axis of the molecule and so the correlation time for this pair might be expected to be more sensitive to rotation around this axis than for other proton pairs. However, there are other proton pairs within the molecule that are also nearly perpendicular to the long axis of the molecule, and NOEs are observed between these at 500 MHz. It is likely in this case that both internal flexibility and anisotropic rotation will contribute to the variations in the effective correlation times.

It is clear that ignoring the effects of local correlation times when using NOEs or ROEs to calculate inter-proton distances will lead to inaccurate results. We have seen such dramatic differences in inter-proton pair correlation times for both terminal and internal glycosidic linkages of oligosaccharides, and similar effects may be expected in other organic molecules. ROEs are less sensitive to these effects than NOEs. However, the most robust method is to measure the local correlations times and use these to calculate corrected distances from either the NOE or ROE data.

Materials and methods

Preparation of oligosaccharides

Glc_3Man*O*Me was synthesised as previously described.[18] $Glc_3Man_7GlcNAc_2$ was purified by lectin affinity chromatography from CHO cells treated with the α-glucosidase inhibitor *N*-butyl deoxynojirimycin as previously described.[17]

NMR spectroscopy

The oligosaccharides samples were repeatedly dried, dissolved in either 500 μl D_2O or CD_3OD and transferred to 5 mm NMR tubes. Proton chemical shifts for samples in D_2O were referenced to acetone at $\delta_H = 2.225$ ppm. Spectra were recorded on Varian UNITY INOVA 500 and 700 spectrometers, with probe temperatures of 30 °C. Two-dimensional spectra were multiplied by sine- or cosine-bell functions in both dimensions, as appropriate. ^1H resonances were assigned from two-dimensional phase-sensitive COSY, RELAY and/or TOCSY spectra. Cross-linkage NOE patterns and comparison of reported assignments for glucosylated oligomannose-type oligosaccharides[17,20] were used for sequence- and stereo-specific assignments. NOE build-up curves were measured to ensure that the mixing time selected for the NOESY and ROESY experiments was in the linear region. All NOESY and ROESY spectra reported were recorded with a mixing time of 200 ms with no random variation. In NOESY spectra, the contribution to the cross-peaks from scalar coupling is dispersive and thus distorts peak shapes without affecting the total peak volume when the spectra are phased correctly.

2D NOESY, ROESY and T-ROESY spectra were all recorded for both samples in D_2O at a ^1H frequency of 500 MHz and for $Glc_3Man_7GlcNAc_2$ in D_2O at a ^1H frequency of 700 MHz. 2D NOESY and ROESY spectra were all recorded for both samples in CD_3OD at 500 MHz. Standard ROESY spectra were recorded with both weak spin-lock fields (approximately 1.5 kHz for both samples) and strong spin-lock fields (2.8 kHz for Glc_3Man*O*Me and 4.3 kHz for $Glc_3Man_7GlcNAc_2$). Absolute volumes of NOE and ROE cross-peaks were measured from the phase-sensitive data using the Varian VNMR 6.1c software. Spectral noise, and thus the error in peak volume measurement, was estimated by measuring the volume integrals of regions of the baseline around the cross-peaks.

Calculation of inter-proton correlation times and distance constraints

Effective correlation times (τ_{ij}) for each proton pair were calculated using the ratio of the NOE cross-relaxation rate to the T-ROE cross-relaxation rate.[10] Distance constraints were calculated from NOE and ROE intensities in the linear build-up region using the two-spin approximation. The internal calibration used to calculate distances was the intra-residue glucose G1:H1–G1:H2 NOE (or ROE). The distance for this proton-pair was obtained from crystallographic data (crystal structure of Glcα1-3Glcα-*O*Me[21]). Two models of the dynamics were used in calculating distances.

Model 1: assume that the correlation time, τ_c, is the same for a pair of protons ij and the reference pair (rigid isotropic motion).

In this case, the NOE or ROE intensity (I) between any pair of protons, i and j, in the linear build-up region (the isolated spin pair approximation) is given by:

$$I_{ij} = \frac{A}{r_{ij}^6}$$

where r_{ij} is the distance between the protons and A is a constant at a given magnetic field strength. A can be determined using the measured value of I for a reference pair of protons of known

separation. Thus:

$$r_{ij} = \sqrt[6]{\frac{I_{ref} \times r_{ref}^6}{I_{ij}}}$$

Model 2: assume that each pair of protons has a different effective correlation time, τ_{ij}, which characterises both the bulk and internal motion for that proton pair.

In this case, the NOE or ROE intensity (I) between any pair of protons, i and j, in the linear build-up region (isolated spin pair approximation) is now given by:

$$I_{ij} = \frac{A_{ij}}{r_{ij}^6}$$

where A_{ij} varies between each proton pair and depends on the effective correlation time for that pair, τ_{ij}:

$$\text{NOE: } A_{ij} = B \times [6J(2\omega)_{ij} - J(0)_{ij}]$$

$$\text{ROE: } A_{ij} = B \times [3J(\omega)_{ij} + 2J(0)_{ij}]$$

$$\text{T-ROE: } A_{ij} = B \times \tfrac{1}{2}[6J(2\omega)_{ij} + 3J(\omega)_{ij} + J(0)_{ij}]$$

where B is a constant, ω is the precession frequency, and the spectral density function J at a frequency υ is given by

$$J(\upsilon)_{ij} = \frac{\tau_{ij}}{1 + (\upsilon\tau_{ij})^2}$$

B can be determined using the measured value of I for a reference pair of protons of known separation and known correlation time. Thus:

$$\text{NOE} : r_{ij} = \sqrt[6]{\frac{I_{ref} \times r_{ref}^6}{I_{ij}} \times \frac{\left[6J(2\omega)_{ij} - J(0)_{ij}\right]}{[6J(2\omega)_{ref} - J(0)_{ref}]}}$$

$$\text{ROE} : r_{ij} = \sqrt[6]{\frac{I_{ref} \times r_{ref}^6}{I_{ij}} \times \frac{\left[3J(\omega)_{ij} + 2J(0)_{ij}\right]}{[3J(\omega)_{ref} + 2J(0)_{ref}]}}$$

$$\text{T-ROE} : r_{ij} = \sqrt[6]{\frac{I_{ref} \times r_{ref}^6}{I_{ij}} \times \frac{\left[6J(2\omega)_{ij} + 3J(\omega)_{ij} + J(0)_{ij}\right]}{[6J(2\omega)_{ref} + 3J(\omega)_{ref} + J(0)_{ref}]}}$$

Acknowledgements

The authors would like to thank Luisa Fernandez Guillen for assistance with Dionex HPLC chromatography, Brian Matthews for performing large scale hydrazinolysis, and David Harvey for mass spectrometry. M.M. is on study leave from Universiti Putra Malaysia and is supported by a scholarship from the Government of Malaysia. This work was also supported by funding from the Oxford Glycobiology Institute.

References

1 D. Neuhaus and M. P. Williamson, *The nuclear Overhauser effect in stereochemical and conformational analysis*, Wiley, New York, Chichester, 2nd edn, 2000.
2 A. A. Bothner-By, R. L. Stephens, J. Lee, C. D. Warren and R. W. Jeanloz, *J. Am. Chem. Soc.*, 1984, **106**, 811–813.
3 A. Bax and D. G. Davis, *J. Magn. Reson.*, 1985, **63**, 207–213.
4 H. Kessler, C. Griesinger, R. Kerssebaum, K. Wagner and R. R. Ernst, *J. Am. Chem. Soc.*, 1987, **109**, 607–609.
5 H. Desvaux, P. Berthault, N. Birlirakis and M. Goldman, *J. Magn. Reson., Ser. A*, 1994, **108**, 219–229.
6 A. Bax, V. Sklenar and M. F. Summers, *J. Magn. Reson.*, 1986, **70**, 327–331.
7 R. Bazzo, C. J. Edge, M. R. Wormald, T. W. Rademacher and R. A. Dwek, *Chem. Phys. Lett.*, 1990, **174**, 313–319.
8 T. L. Hwang and A. J. Shaka, *J. Am. Chem. Soc.*, 1992, **114**, 3157–3159.
9 T. L. Hwang and A. J. Shaka, *J. Magn. Reson., Ser. B*, 1993, **102**, 155–165.
10 A. Poveda, J. L. Asensio, M. Martin Pastor and J. Jimenez Barbero, *Carbohydr. Res.*, 1997, **300**, 3–10.
11 S. W. Homans, R. A. Dwek and T. W. Rademacher, *Biochemistry*, 1987, **26**, 6553–6560.
12 T. Weimar and R. J. Woods, Combining NMR and simulation methods in oligosaccharide conformational analysis, in *NMR Spectroscopy of Glycoconjugates*, ed. J. Jimenez-Barbero and T. Peters, Wiley-VCH, Weinheim, 2003; pp. 111–144.
13 A. Helenius and M. Aebi, *Science*, 2001, **291**, 2364–2369.
14 J. D. Schrag, D. O. Procopio, M. Cygler, D. Y. Thomas and J. J. Bergeron, *Trends Biochem. Sci.*, 2003, **28**, 49–57.
15 E. W. Wooten, C. J. Edge, R. Bazzo, R. A. Dwek and T. W. Rademacher, *Carbohydr. Res.*, 1990, **203**, 13–17.
16 M. R. Wormald and C. J. Edge, *Carbohydr. Res.*, 1993, **246**, 337–344.
17 A. J. Petrescu, T. D. Butters, G. Reinkensmeier, S. Petrescu, F. M. Platt, R. A. Dwek and M. R. Wormald, *EMBO J.*, 1997, **16**, 4302–4310.
18 S. C. Ennis, I. C. Cumpstey, A. J. Fairbanks, T. D. Butters, M. Mackeen and M. R. Wormald, *Tetrahedron*, 2002, **58**, 9403–9411.
19 R. J. Woods, A. Pathiaseril, M. R. Wormald, C. J. Edge and R. A. Dwek, *Eur. J. Biochem.*, 1998, **258**, 372–386.
20 E. Alvarado, T. Nukada, T. Ogawa and C. E. Ballou, *Biochemistry*, 1991, **30**, 881–886.
21 A. Neuman, D. Avenel, F. Arene, H. Gillier-Pandraud, J.-R. Pougny and P. Sinay, *Carbohydr. Res.*, 1980, **80**, 15–24.

